

OPEN ACCESS

Hydrothermal synthesis, off-axis electron holography and magnetic properties of Fe_3O_4 nanoparticles

To cite this article: Trevor P Almeida *et al* 2014 *J. Phys.: Conf. Ser.* **522** 012062

View the [article online](#) for updates and enhancements.

You may also like

- [Imaging of magnetic and electric fields by electron microscopy](#)
Josef Zweck
- [In situ off-axis electron holography of real-time dopant diffusion in GaAs nanowires](#)
Ganapathi Prabhu Sai Balasubramanian, Elizaveta Lebedkina, Nebile Isik Goktas et al.
- [Correlative investigation of Mg doping in GaN layers grown at different temperatures by atom probe tomography and off-axis electron holography](#)
Lynda Amichi, Isabelle Mouton, Victor Boureau et al.

ECS
The
Electrochemical
Society
Advancing solid state &
electrochemical science & technology

DISCOVER
how sustainability
intersects with
electrochemistry & solid
state science research

Hydrothermal synthesis, off-axis electron holography and magnetic properties of Fe₃O₄ nanoparticles

Trevor P. Almeida,^{1*} Adrian R. Muxworthy¹, Wyn Williams², Takeshi Kasama³
and Rafal E. Dunin-Borkowski⁴

¹Department of Earth Science and Engineering, South Kensington Campus, Imperial College London, London, SW7 2AZ, UK.

²School of GeoSciences, University of Edinburgh, Edinburgh, EH9 3JW, UK.

³Centre for Electron Nanoscopy, Technical University of Denmark, DK-2800 Kongens Lyngby, Denmark

⁴Ernst Ruska-Centre for Microscopy and Spectroscopy with Electrons and Peter Grünberg Institute, Forschungszentrum Jülich, D-52425 Jülich, Germany.

Abstract. The hydrothermal synthesis of Fe₃O₄ nanoparticles (NPs) (< 50 nm) from mixed FeCl₃ / FeCl₂ precursor solution at pH ~ 12 has been confirmed using complementary characterisation techniques of transmission electron microscopy and X-ray diffractometry. Off-axis electron holography allowed for visualisation of their single domain (SD) nature, as well as inter-particle interactions, with the latter attributed to explain the pseudo-SD/multi-domain behaviour demonstrated by bulk magnetic measurements.

1. Introduction

The ability of a rock to reliably record the geomagnetic field depends on the geometry and size of the constituent magnetic particles, whereby large or closely packed grains that have large magnetostatic interactions between them will affect their recording fidelity [1]. Generally, particles in the single domain (SD) grain size range (< 100 nm) are regarded as ideal palaeomagnetic recorders because of their strong remanence and high magnetic stability, with potential relaxation times greater than that of the age of the Universe [2]. However, rocks rarely contain ideal assemblages of mono-dispersed SD particles and techniques used to determine the magnetic domain state of remanence carriers often reveal the presence of very small superparamagnetic (SP) particles, i.e., nanometric, plus pseudo-single domain (PSD) and multi-domain (MD) particles. As the magnetic minerals in rocks commonly show broad variations in particle size, shape and spacing, synthetic analogues are considered more ideal for study.

Magnetite (Fe₃O₄) is arguably the most important naturally occurring magnetic naturally mineral on Earth [3]. Understanding its grain size behaviour and recording fidelity is crucial to palaeomagnetism. Previously nano-sized Fe₃O₄ have been prepared by various methods such as sol-gel processing, hydrothermal synthesis, forced hydrolysis, ball milling and microemulsion. In this paper, we consider the approach of hydrothermal synthesis (HS), which in particular, offers effective control over the size and shape of Fe₃O₄ nanoparticles (NPs) at relatively low reaction temperatures and short reaction times, providing for well-crystallised reaction products with high homogeneity and definite composition [4]. Off-axis electron holography permits nanometre-scale imaging of magnetic induction within and around materials as a function of applied field and temperature [3, 5]. In this context, the HS of Fe₃O₄ NPs is presented, and comparison of their magnetic properties investigated using off-axis electron holography and more conventional rock magnetism technique was made.

* Author to whom correspondence should be addressed: t.almeida@imperial.ac.uk.



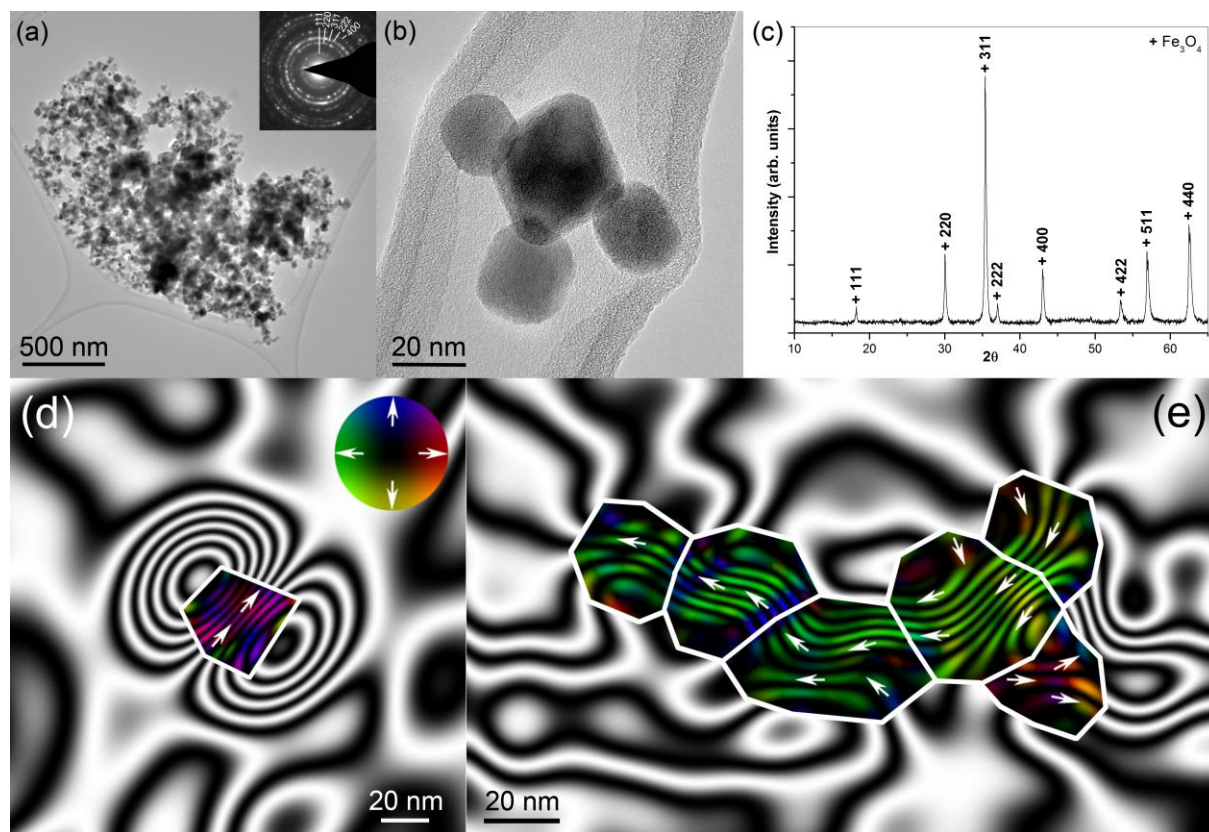


Figure 1 BF TEM images of (a) a large group of Fe_3O_4 NPs, as identified by SAED pattern (inset, indexed to Fe_3O_4 (JCPDS 88-0315)); and (b) a few individual Fe_3O_4 NPs. (c) Associated XRD pattern of the synthesised NPs, confirming the Fe_3O_4 phase. (d) Magnetic induction map of an individual Fe_3O_4 NP in the SD size range (~ 45 nm) acquired in magnetic field-free conditions and determined from the magnetic contribution to the phase shift reconstructed from off-axis electron holograms, revealing the SD nature of the particle. Magnetisation direction is depicted in the colour wheel (inset). (e) Magnetic induction map of a group of Fe_3O_4 NPs, showing magnetic contours flowing through the SD particles. The contour spacings are (d) 0.029 and (e) 0.049 radians.

2. Experimental

For the HS of Fe_3O_4 , 0.2 ml FeCl_3 aqueous solution (45% pure FeCl_3 ; Riedel-de Haen, Germany) and 150 mg FeCl_2 powder (98.0% CoCl_2 ; Sigma-Aldrich, UK) were further diluted in 40 ml distilled water and mechanically stirred in a 125 ml Teflon-lined steel autoclave. The precursor solution was adjusted to pH ~ 12 with the drop-wise addition of aqueous NaOH solution, then sealed and inserted into a temperature controlled furnace at 200°C for 3 hours. The autoclave, once removed from the furnace, was allowed to cool down to room temperature naturally.

The synthesised reaction products were centrifuged for 5 minutes at 5000 rpm, cleaned with acetone and deposited onto single crystal silicon substrates for the purpose of structural characterisation using a PANalytical X'Pert PRO Diffractometer ($\text{CuK}\alpha$ radiation; $\theta/2\theta$ diffraction geometry). For the purpose of transmission electron microscopy (TEM) investigation, the acetone cleaned HS suspensions were dispersed using an ultrasonic bath before deposition onto lacey carbon / copper mesh support grids (Agar Scientific Ltd, UK). Conventional bright field (BF) imaging was performed using a FEI Tecnai TEM operated at 200 kV (Centre for Electron Nanoscopy (CEN), Technical University of Denmark) and selected area electron diffraction (SAED) allowed for phase identification. For off-axis electron holography, a FEI Titan TEM fitted with a C_s corrector on the condenser lens, and a Lorentz lens and biprism, was used at 300kV (CEN).

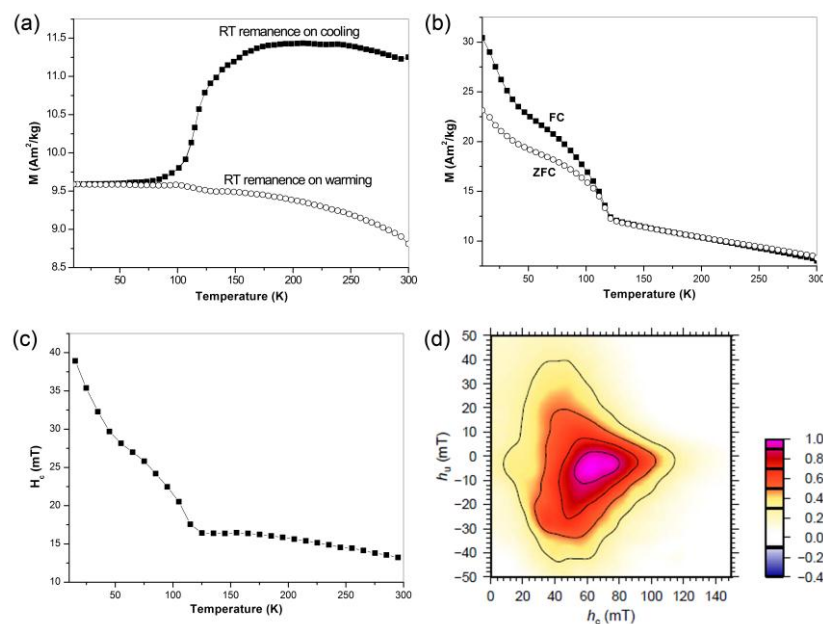


Figure 2 (a) RT-SIRM cycling curves; and (b) ZFC-FC magnetisation measurements of the Fe_3O_4 NPs; (both measured from 10 – 300 K). (c) H_c versus temperature (15–295 K) measurement and (d) normalized ZFC FORC diagram acquired at 15 K (smoothing factor = 2).

For the purpose of magnetic measurements, a dry powdered sample was inserted, compressed and sealed in a plastic pellet and examined at the Institute for Rock Magnetism (I.R.M) at the University of Minnesota, Minneapolis, USA. Low-temperature hysteresis measurements from 15 – 295 K (in 10 K intervals), and first-order reversal curve (FORC), at 15 K, were made using a Princeton Measurements Vibrating Sample Magnetometer (VSM). A Quantum Designs Magnetic Properties Measuring Systems (MPMS) cryogenic magnetometer was used to measure cooling and warming curves of room temperature (RT) induced saturation isothermal remanence magnetisation (SIRM) to identify low-temperature crystallographic transitions. In addition, warming curves of SIRM at 10 K after field cooling (FC) at 2.5 T and zero-field cooling (ZFC) from 300 K to 10 K, were made.

3. Results

The hydrothermal processing of mixed $\text{FeCl}_3 / \text{FeCl}_2$ precursor solution led to the synthesis of a nano-structured Fe_3O_4 reaction product, the evidence for which is now presented in detail.

Fig. 1 provides information on the morphology, size and structure of the synthesised Fe_3O_4 NPs. The BF TEM image of Fig. 1a presents the HS reaction product and is shown to comprise crystalline Fe_3O_4 NPs, as identified by SAED (inset), which exhibit some faceting but are generally isotropic and < 50 nm in size (Fig. 2b). The peaks in the XRD pattern of Fig. 1c are in good agreement with the formation of Fe_3O_4 (Joint Committee on Powder Diffraction standards (JCPDS) reference 88-0315).

The magnetic induction map of an individual Fe_3O_4 NP (~ 45 nm) presented in Fig. 1d, determined from the magnetic contribution to the phase shift reconstructed from electron holograms, depicts the magnetic field contours to be concentrated to – and flow diagonally right and upward through – the centre of the Fe_3O_4 NP, as well as a stray magnetic field expected for a SD particle. Fig. 1e shows magnetic induction map of a group of Fe_3O_4 NPs, displaying the magnetic contours to again flow through the SD particles, and the expected stray magnetic field.

Fig. 2 provides information on the magnetic properties of the Fe_3O_4 NPs. The low-temperature SIRM cycling curves (Fig. 2a) displays behaviour typically reported for PSD magnetite with a Verwey transition of ~ 120 K; however, theoretical models also predict such behaviour for SD particles at this temperature [6]. The drop in the remanence at the Verwey transition suggests that part of the magnetic remanence is carried by interacting SD and/or small PSD (vortex) domain states.

Low-temperature warming of SIRM to 10K (Fig. 2b), clearly reveals the Verwey transition, and is indicative of near stoichiometric magnetite. The hysteresis parameter of coercivity (H_C) is plotted as a function of temperature (15 K to 295 K) in Fig. 2c and displays H_C behaviour typical of SD or small PSD magnetite [7], i.e., on warming H_C drops at 15K, until the Verwey transition, followed by a gradual drop from 16 to 13 mT on warming to room temperature; such behaviour has been previously predicted [8]. The FORC diagram of Fig. 2d was measured at 15 K after ZFC and exhibited behaviour characteristic of SD grains displaying moderate inter-particle magnetostatic interactions [9].

4. Discussion

This TEM and XRD investigation of the HS of mixed $\text{FeCl}_3 / \text{FeCl}_2$ precursor solution, at pH ~ 12 , has provided evidence for the development of Fe_3O_4 NPs that are generally isotropic and < 50 nm in size. A HS reaction temperature of 200°C was observed sufficient to promote the formation of the thermodynamically stable Fe_3O_4 iron oxide phase as the sole reaction product, whilst it is considered that the Fe_3O_4 NP growth mechanism may have involved the growth and dissolution of intermediate iron (oxy)hydroxide phases. Kinematically accessible amorphous $\text{Fe}(\text{OH})_3$, poorly crystalline 'hydroxychloride green rust 1': $\text{Fe}_{3.6}\text{Fe}_{0.9}(\text{O}, \text{OH}, \text{Cl})_9$ (JCPDS 13-88) sheets and $\alpha\text{-FeOOH}$ nanorods are known to precipitate during HS at relatively low temperatures in iron-chloride salt solutions at pH ~ 12 [4, 10], and their dissolution with increasing temperature is considered to supply elemental growth constituents for formation of the more thermodynamically stable Fe_3O_4 .

Complementary hysteresis and thermomagnetometry combined with off-axis electron-holography measurements, provided information on the magnetic properties of the Fe_3O_4 NPs. The magnetic induction map of an individual Fe_3O_4 NP (Fig. 1d) demonstrates its SD behaviour, as evidenced by the uniaxial magnetic contours concentrated to the NP centre and stray magnetic field. This is reinforced by the FORC diagram that exhibits behaviour characteristic of interacting single-domain grains. However, the H_c , RT-SIRM and ZFC-FC cycling data reveals behaviour more indicative of PSD/MD domain-states. Considering the HS reaction product is in a powdered form, the PSD/MD-like behaviour is suggested to be caused by inter-particle interaction of the Fe_3O_4 NPs during measurement [11], which is supported by the visualised interactions between the SD particles shown in Fig. 1e and the FORC data (Fig. 2d).

In summary, complementary TEM and XRD have confirmed the HS of SD Fe_3O_4 NPs (< 50 nm in diameter). Off-axis electron holography showed their SD nature and explained the PSD/MD behaviour demonstrated by the bulk magnetic measurements through visualisation of inter-particle interactions.

References

- [1] Krasa D, Wilkinson C D W, Gadegaard N, Kong X, Zhou H, Roberts A P, Muxworthy A R and Williams W 2009 *J. Geophys. Res.* **163**, 243.
- [2] Dunlop D J and Ozdemir O, 1997 *Rock Magnetism: Fundamentals and Frontiers*, (Cambridge Univ. Press, Cambridge, U.K.)
- [3] Harrison R, Dunin-Borkowski R E and Putnis A 2002 *PNAS* **99**, 16556-16561.
- [4] Zheng Y, Cheng Y, Bao F and Wang Y 2006 *Mater. Res. Bull.* **41**, 525-529.
- [5] Dunin-Borkowski R E, McCartney M R, Frankel R B, Bazylinski D A, Posfai M and Buseck P R 1998 *Science* **282**, 1868-1870.
- [6] Muxworthy A R and Williams W 2006 *J. Geophys. Res.* **111**, B07103.
- [7] Schmidbauer E and Keller R 1996 *J. Magn. Magn. Mater.* **152**, 99-108.
- [8] Carter-Stiglitz B, Jackson M and Moskowitz B 2002 *Geophys. Res. Lett.* **29**, NO. 7, 10.1029/2001GL014197.
- [9] Muxworthy A, Heslop D and Williams W 2004 *Geophys. J. Int.* **158**, 888-897.
- [10] Almeida T P, Fay M W, Zhu Y Q and Brown P D 2012 *J. Phys. Conf. Ser.* **371**, 012074.
- [11] Muxworthy A R, Williams W and Virdee D 2003 *J. Geophys. Res.* **108**, 2517.

Acknowledgements

This project was primarily funded by NERC grant NE/H00534X/1, with additional funding from Institute for Rock Magnetism, University of Minnesota, USA, which is funded by the W. M. Keck Foundation, The National Science Foundation, and the University of Minnesota.